Food & Function

PAPER

Check for updates

Microalgae oil from *Schizochytrium* sp. alleviates obesity and modulates gut microbiota in high-fat diet-fed mice†

Liyuan Ran,[a] Jinhui Yu,[b,c,d] Rui Ma,[b,c] Qing Yao,[b,c] Mingjie Wang,[e,f] Yuping Bi,[d] Zichao Yu [ID] *[a] and Yingjie Wu*[a,b,c]

Omega-3 PUFAs rich in fish oil are believed to prevent obesity by improving lipid metabolism and regulating gut microbiota. Microalgae oil is considered as an alternative source of omega-3 PUFAs owing to diminishing fish resources. *Schizochytrium* microalgae oil (SMO), with a high DHA proportion, is a promising source for commercial DHA production. However, its weight-loss and gut microbiota-regulating properties are not well studied. Here we compared the obesity reducing effects of SMO, commercial fish oil (FO) and a weight-loss drug, Orlistat (OL), in a high-fat diet (HFD) induced obesity mouse model. We found that SMO is comparable to commercial FO and OL with regard to weight loss, and it even exhibits the weight-loss effects earlier than FO and OL. It can efficiently inhibit the expression of lipogenesis-related genes and induce the expression of lipolysis-related genes. Moreover, SMO has different gut microbiota modulating effects from those of FO and OL. It does not influence the diversity of bacterial community, but does increase the abundance of several beneficial SCFAs-producing bacteria and inhibits obesity-promoting *Desulfovibrio* and several pathogens. We also found that SMO recovers the HFD-disturbed metabolic capability of gut microbiota. It can increase the abundance of several metabolism-related pathways, such as those of amino acids, SCFAs and bile acid, and decrease the level of the LPS biosynthesis pathway, which probably contributes to an improvement of lipid metabolism and restoration of the colonic mucosal barrier impaired by HFD. Our data suggest that SMO can be used as a superior dietary supplement for alleviating obesity.

1. Introduction

Obesity has been a growing public health concern. It is associated with a high risk of several adverse diseases, including cardiovascular disease, type 2 diabetes, liver disease, kidney disease, and various cancers.[1–4] Many strategies have been developed to prevent and alleviate obesity, including dietary control, exercise, surgical treatment, and medication.[5] Anti-obesity drugs, such as Orlistat, have modest clinical efficacy but severe side effects.[6] Therefore, dietary intervention has been considered a relatively safe, easy and convenient method to attenuate obesity. In addition, anti-obesity foods derived from natural materials are generally preferred for safer long-term treatment over drugs.

Omega-3 polyunsaturated fatty acids (PUFAs), including eicosapentaenoic acid (EPA; 20:5n-3) and docosahexaenoic acid (DHA; 22:6n-3), have been proven to prevent the development of obesity in rodents and humans. They can ameliorate obesity by suppressing hepatic lipogenesis and steatosis and inhibit the differentiation of adipocytes.[7,8] Dietary EPA and DHA have been primarily derived from marine fish oils. However, harvesting marine fish is often hampered by many factors, such as seasonal variation and environmental pollution. Fish oil resources will not be adequate due to rapidly increasing demands and reductions in fish production resulting from the deterioration of marine environments. As a result, microalgae that exhibit advantages in terms of high

[a]*College of Laboratory Animals (Shandong Laboratory Animal Center), Shandong Provincial Hospital, Medical Science and Technology Innovation Center, Shandong First Medical University & Shandong Academy of Medical Sciences, Jinan, 250117, China. E-mail: zcyu@sdfmu.edu.cn, yjwu@sdfmu.edu.cn*
[b]*Institute of Genome Engineered Animal Models for Human Diseases, Dalian Medical University, Dalian, 116044, China*
[c]*National Center of Genetically Engineered Animal Models for International Research, Dalian Medical University, Dalian, 116044, China*
[d]*Institute of Crop Germplasm Resources, Shandong Academy of Agricultural Sciences, Jinan, 250100, China*
[e]*Shandong Provincial Hospital, Shandong University, Jinan, China*
[f]*Department of Endocrinology, Affiliated Hospital of Inner Mongolia Medical University, Inner Mongolia Medical University, Inner Mongolia, China*
†Electronic supplementary information (ESI) available. See DOI: https://doi.org/10.1039/d2fo01772e

content of PUFAs, controllability and sustainability have attracted attention as alternative sources of omega-3 PUFA. Accumulating studies have revealed the anti-obesity effects of microalgae oils. DHA from *Crypthecodinium cohnii* reduces the VLDL TG and total TG levels and increases the concentration of IL-10 in the plasma of obese adults.[9] Oil from *Thraustochytriidae* sp. was reported to induce weight loss and inhibit hepatic lipid accumulation in high-fat-induced obese mice.[10] Obese mice treated with microalgae oil from *Aurantiochytrium* sp. KRS101 displayed a significant decrease in body weight gain, epididymal fat pad weight, serum TG, total cholesterol level, and the expression of lipogenesis-related stearoyl-CoA desaturase enzyme 1 (SCD1).[11] Besides the above microalgae, the heterotrophic marine microalgae *Schizochytrium* sp. with a high DHA proportion in their total fatty acid profile has been a promising source for commercial DHA production. Oil from *Schizochytrium* sp. (SMO) has been authorized by the European Commission to be used as a novel food ingredient. It was found that SMO is able to reduce the plasma TG level and the low-grade inflammation in high-fat-induced obese rats.[12,13] In addition, the preventative effects of SMO on obesity were revealed in our previous study using a mouse model.[14] However, the weight-reducing effects of SMO on high-fat-induced obesity are still unclear.

Gut microbiota are of significant importance for host's health, which is essential for the host's nutrition, metabolism, immunity, and development.[15] Increasing evidence has revealed that the dysbiosis of gut microbiota is tightly associated with the development of obesity and metabolic disorders in both mice and humans.[16] Therefore, gut microbiota can serve as potential targets for developing therapies for obesity. For example, certain beneficial bacterial species, such as *Bifidobacterium* spp. and *Akkermansia muciniphila*, were proved to improve obesity.[17] Dietary omega-3 PUFAs were demonstrated to alter the gut microbiota in mice and humans.[18] However, the effects of SMO on gut microbiota were unclear.

In the present study, HFD-induced obese mice were treated with SMO. The weight-reducing and gut microbiota modulation effects of SMO on obese mice were assessed, using fish oil and Orlistat as positive controls. Our results may lay valuable groundwork for developing safe, functional food supplements or drugs for alleviating obesity.

2. Materials and methods

2.1. Reagents

A regular chow diet (RC, D12450J, 19.2% g protein, 67.3% g carbohydrate, 4.3% g fat, and 10% kcal from fat) and a high-fat diet (HFD, D12492, 26.2% g protein, 26.3% g carbohydrate, 34.9% g fat, and 60% kcal from fat) were purchased from Research Diets (New Brunswick, USA). Microalgae oil from *Schizochytrium* sp. was purchased from Tiankai Biological Technology Co., Ltd (Jiangsu, China). It was purified by using a high voltage glass column (C18 70 × 460 mm^2) in a medium pressure rapid preparation system (Flash, Biotage, USA) under

the purification conditions described previously.[14] The purified oil was denoted as SMO. Fish oil (FO, Nature's Bounty, Long Island, USA) and Orlistat (OL, Aladdin, Shanghai, China) were used as positive controls to analyze the anti-obesity effect of SMO. The fatty acid compositions of SMO and FO are listed in Table S1.† DHA was dominant in SMO (97.8%), and the proportion of EPA as well as saturated fatty acids (SFAs) and monounsaturated fatty acids (MUFAs) was as low as 1%. In the FO, SFAs were the most abundant (38.3%), and the content of DHA (16.7%) and EPA (19.3%) was almost the same.

2.2. Animals and experimental design

As shown in Fig. S1A,† weaning male C57BL/6J mice that were four weeks old were randomly divided into regular chow (RC) and high-fat diet (HFD) groups. They were maintained in a temperature- and humidity-controlled room with a 12 h light/dark cycle at the Specific Pathogen Free Experimental Animal Center of Dalian Medical University. The mice in the two groups were treated for eight weeks to construct the HFD-induced obesity mouse model. Then, the mice in the HFD group were randomly divided into four sub-groups: (a) the HF group fed with HFD; (b) the FO group fed with HFD and FO; (c) the SMO group fed with HFD and SMO; and (d) the OL group fed with HFD and OL (40 mg per kg body weight). The gavage dosages of FO and SMO were unified as 100 mg of omega-3 PUFAs per kg body weight adjusted by medical-grade corn oil (Aladdin, Shanghai, China) to keep it isovolumetric. The RC, HF and OL groups were administered with isovolumetric corn oil. All of the groups were treated for 16 weeks before sacrifice. All animal experiments were performed under the guidelines for the treatment of laboratory animals and were approved by the Committee on the Ethics of Animal Experiments of Dalian Medical University.

2.3. Glucose tolerance and insulin tolerance tests

At the end of the experiment, the glucose tolerance test (GTT) and insulin tolerance test (ITT) were performed as described previously.[19] Briefly, 2 g kg^{-1} glucose (Sigma Aldrich, Saint Louis, MO) was injected intraperitoneally into overnight-fasted mice for GTT. The blood glucose levels were measured at 0, 30, 60, 90 and 120 min after glucose injection with an automated glucometer (Roche, Basel, Switzerland). For ITT, 0.75 international units (IU) per kg insulin (Humulin R, Eli Lily, Indianapolis, IN) was injected intraperitoneally into mice that were fasted for 4 h and blood levels were measured at 0, 15, 30, 45, and 60 min after insulin injection. The area under the curve (AUC) was calculated as described previously.[20]

2.4. Collection of the analyzed samples

At the end of the experiment, tissue and blood samples were collected. The liver, white adipose tissue (located in the epididymal, mesenteric, perinephric, and inguinal regions), and brown adipose tissue (located in the subscapular) were dissected. After being weighed, partial liver and subcutaneous fat were fixed with 10% formalin for histological observation, and the residual samples were snap-frozen in liquid nitrogen

before storage at −80 °C. Serum was separated from whole blood by centrifugation at 1000*g* for 10 min at 4 °C and stored at −80 °C for further use. Colon contents were collected from each mouse and then snap-frozen immediately and stored at −80 °C for gut bacterial community analysis.

2.5. Body weight, organ weight and serum analysis

For each mouse body weight was recorded every two weeks during the experimental period. The liver and the fat were weighed at the end of the experiment using an analytical balance. The triglyceride (TG) and total cholesterol (T-CHO) contents in the serum were measured using TG and T-CHO test kits (A110-1 and A111-1, Jian Cheng Biological Engineering Institute, Nanjing, China) according to the manufacturer's instructions.

2.6. Protein extraction and Western blot

Proteins were extracted from the frozen fat and colon with RIPA lysis buffer (R0020, Solarbio, Beijing, China) containing a protease inhibitor cocktail (P1006, Beyotime, Shanghai, China). Protein contents were measured by using a BCA assay kit (P0012, Beyotime, Shanghai, China), and samples were diluted accordingly to normalize the protein content to 25 μg per well for SDS-PAGE separation. The separated proteins were transferred onto a nitrocellular membrane for probing with the indicated antibodies. The membrane was blocked with TSBT buffer (50 mmol L^{-1} Tris-HCl, 150 mmol L^{-1} NaCl and 1‰ Tween 20) containing 5% skim milk at room temperature for 1 h and then incubated with the diluted primary antibody at 4 °C overnight. After extensive washing with TSBT, the membrane was incubated with HRP-labelled goat-anti-rabbit IgG antibody (Proteintech, Chicago, IL) at room temperature for 1 h. After final washing with TSBT, the membrane was incubated in a Western lighting-ECL substrate system (Proteintech) and exposed to an automatic chemiluminescence gel imaging system (Bio-Rad, Hercules, CA). The following primary antibodies were used in this study: ATGL (55190-1-AP, Proteintech), HSL (ABP51575, Abbkine, Wuhan, China), FASN (10624-2-AP, Proteintech), Occludin (A12621, ABclonal, Wuhan, China), Claudin-1 (A21949, ABclonal), and GAPDH (10494-1-AP, Proteintech).

2.7. Hematoxylin–Eosin (H&E) staining

Liver, fat and colon tissues were fixed with 10% formalin for at least 24 h. Samples were sliced into 5 μm sections after embedding in paraffin and then stained with H&E. Digital images were captured with a Nikon NI-E light microscope (Nikon, Tokyo, Japan).

2.8. Analysis of the gut bacterial community

The cecal content samples from three individuals were pooled together for DNA extraction and high throughput sequencing. Thus, there were three replicates for each group. The total DNA in the cecal contents was extracted using an E.Z.N.A. stool DNA isolation kit (OMEGA Bio-tek, Norcross, GA) according to the manufacturer's instructions. Sequencing of the hypervariable regions V3–V4 of the bacterial 16S rRNA gene was per-

formed using the Illumina MiSeq platform from Majorbio Biopharm Technology Co., Ltd (Shanghai, China). Data analysis was done using QIIME2 to analyze the diversity and taxonomic composition of the bacterial community.[21] Briefly, the paired-end reads were denoised and stitched, and an operational taxonomic unit (OTU) table was generated along with representative sequences. In the diversity analysis, the sequence counts of each sample in the OTU table were subsampled to the minimum count of all the samples to avoid bias caused by different sequencing depths. The taxonomy of each representative sequence was annotated by the Sklearn classifier algorithm against the Silva database version 132 (99% OTU dataset). Alpha diversity metrics, including the Chao1 and Pielou evenness indexes, were calculated with the diversity plugin in QIIME2. The constrained principal coordinate analysis (CPCoA) constrained by the different treatments was performed in R to evaluate the differences in bacterial community based on the Bray–Curtis distance. The pairwise Pearson's correlations between the OTUs and the obesity-related indexes, including body weight gain, brown and white adipose tissue weights, liver weight, and serum glucose, GTT, ITT, T-CHO, and TG levels, were calculated and visualized by using the psych and pheatmap packages in R software.

2.9. Prediction of the bacterial community phenotypes and functions

The high-level phenotypes of the bacterial community were predicted using BugBase.[22] The annotated OTU matrix was uploaded to the website (**https://bugbase.cs.umn.edu/**), and the microbiome phenotypes were predicted, including oxygen utilization, Gram positive, and Gram negative. The functional capabilities of the bacterial community were predicted using the Tax4Fun2 package[23] in R software based on the OTUs and the representative sequences obtained by QIIME2. The Kyoto Encyclopedia of Gene and Genomes (KEGG) database was used as the reference, and KEGG Orthologs (KOs) were predicted based on the relative abundance of all the OTUs. The KEGG pathway abundance was consequently inferred based on the abundance of KOs. A linear discriminant analysis (LDA)[24] was performed to identify the significantly distributed functional pathways among the different groups, and the relative abundance and distribution of these pathways were visualized by a heatmap.

2.10. Statistical analyses

The values in this study were expressed as means ± SEM. Statistical Package for Social Sciences (SPSS) 19.0 (SPSS INC, Chicago, IL, USA) was used for the statistical analysis. Statistical analysis was performed by one-way analysis of variance followed by the least significant difference *post hoc* test. The statistical significance threshold was set at $P < 0.05$.

3. Results

3.1. Construction of the obesity mouse model

In this study, an obesity mouse model was established by HFD induction to investigate the weight-reducing effects of SMO.

Four-week-old mice were randomly divided into regular chow (RC) and HFD groups (Fig. S1A†). After feeding with HFD for eight weeks, body weights of mice in the HFD group were significantly higher than those of mice in the RC group (Fig. S1B†). In addition, a GTT test revealed that HF mice were glucose intolerant (Fig. S1C and D†). These results indicated that an obesity mouse model was successfully established.

3.2. Effects of SMO on glucose and lipid homeostasis

GTT and ITT assays revealed that mice treated with FO, SMO and OL responded better to a glucose challenge and were more sensitive to insulin stimulation than mice in the HF group (Fig. 1A and B). The fasting blood glucose level was significantly higher in the HF group than in the RC group (HF 190.4 ± 15.48 mg dL^{-1} vs. RC 128.9 ± 16.08 mg dL^{-1}). They
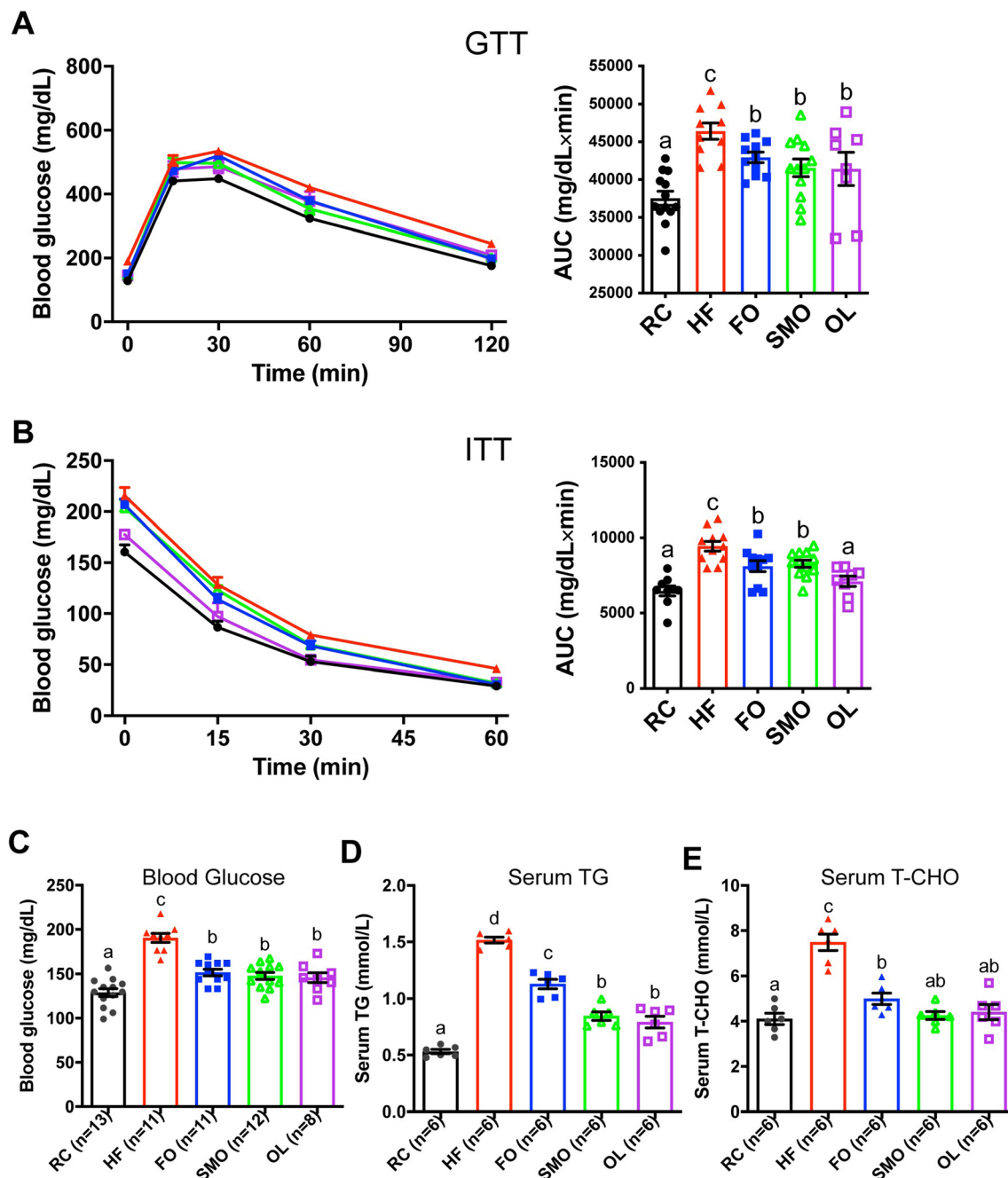

Fig. 1 Effects of SMO on GTT, ITT, and glucose and lipid homeostasis. (A) GTT was measured at the end of the treatment. Inset: the area under the curve in GTT. (B) ITT was measured at the end of the treatment. Inset: the area under the curve in ITT. (C) Fasting blood glucose level of each group. (D) Serum TG level of each group. (E) Serum T-CHO level of each group. Different lowercase letters above the error bars indicate significant differences among groups.

were all significantly lower in the FO (151.53 ± 12.39 mg dL^{-1}), SMO (147.75 ± 13.85 mg dL^{-1}) and OL groups (145.8 ± 15.78 mg dL^{-1}) than in the HF group, although they were still higher than that in the RC group (Fig. 1C). Serum TG level in the HF group was significantly higher than that in RC mice (1.52 ± 0.06 mmol L^{-1} *vs.* 0.53 ± 0.05 mmol L^{-1}). After treatment with FO, SMO and OL, the serum TG levels were all significantly reduced compared with the HF group, and the TG levels were significantly lower in the SMO and OL groups than that in the FO group (Fig. 1D). The trend in serum T-CHO level was similar to the TG level. Serum T-CHO level in HF mice was significantly elevated when compared with that of RC mice (7.48 ± 0.89 mmol L^{-1} *vs.* 4.1 ± 0.62 mmol L^{-1}) and it was reduced to the RC level in the SMO and OL groups (Fig. 1E), while it was still higher in the FO group than in the RC group.

3.3. Effects of SMO on body weight and lipid accumulation in HFD-induced obesity mice

The growth curves showed that the body weights of mice in the SMO group were significantly lower than those in the HF group from the second week post administration, while a significant reduction in body weight gain was observed four weeks and six weeks post administration of OL and FO, respectively (Fig. 2A). In addition, the weight gain of mice was significantly lower in all the groups treated with oils and Orlistat than in the HF group after 16 weeks of treatment, while OL was most effective (Fig. 2B). After the obese mice were treated for 16 weeks, anatomical dissections revealed that the heavier body weight in HF mice was mainly due to more weight gain in the adipose tissues and liver (Fig. 2C–H). The HFD resulted in an evident increase in the weights of both brown adipose tissue (BAT) and white adipose tissue located in the subcutaneous (SubQ), epididymal (Epi), perinephric (Peri) and mesenteric (Mes) regions, and SMO, fish oil and Orlistat significantly reduced their weights (Fig. 2C–G). The weight of the liver was significantly increased in the HFD-induced obesity mouse, and both SMO and OL reduced it to the RC level, while the liver weight in the FO group was still heavier than that in the RC group (Fig. 2H). H&E staining showed that the size of adipocytes in the SubQ WAT of HFD-fed mice was significantly larger than that of the RC group, whereas FO, SMO and OL treatments significantly reduced the size of adipocytes (Fig. 2I). A significant increase in hepatic steatosis marked by vacuolated and lipid-laden hepatocytes was observed in the HF group. Both SMO and OL treatment significantly reduced the degree of fatty liver, while it was only partially remitted in the FO group (Fig. 2I).

3.4. Effects of SMO on lipid metabolism in HFD-induced obesity mice

Western blot analysis was performed to check the expressions of proteins related to lipogenesis and lipolysis in the adipose tissues (Fig. 3). The expression of the lipolysis-related gene adipose triglyceride lipase (ATGL) was higher in the HF group than in the RC group. It was significantly higher in the SMO group than in the HF group, and fish oil

and Orlistat slightly induced ATGL expression without significant difference compared to the HF group. The expression of hormone-sensitive lipase (HSL) involved in lipolysis was similar among all five groups. The expression of fatty acid synthase (FASN) was the lowest in the SMO group, and there was no significant difference among the other four groups. Overall, the SMO group showed an obvious lowest lipogenesis-related gene expression and highest lipolysis-related gene expression in the adipose tissues of the three oil- and drug-treated groups.

3.5. The alpha-diversity and beta-diversity of the gut bacterial community

The alpha-diversity of the bacterial community was indicated by the Chao1 richness index that is based on the estimated number of OTU species (Fig. 4A) and the Pielou evenness index that measures the uniformity of the abundance of different species (Fig. 4B). The Chao1 index was the lowest in the FO group despite there being no significant difference. The Pielou index did not vary significantly among the RC, HF, SMO, and OL groups. However, it was significantly lower in the FO group than in the RC, HF, and SMO groups. The beta-diversity of the bacterial communities was revealed by CPCoA analysis to assess the effect of different treatments on the profile of gut bacterial communities (Fig. 4C). The diet treatments explained 39.7% of the overall variance in the bacterial community. Apparent clustering of the bacterial communities was observed among the samples, and samples from the same group were separated from other groups. Moreover, the distance between the HF and RC groups was closer than those between the HF group and any other group. These results suggested that FO, SMO and OL all altered the structure of the gut bacterial community, but their influences on it were different.

3.6. Taxonomic composition of the gut bacterial community under different treatments

The gut bacterial community was dominated by the phyla *Bacteroidetes* and *Firmicutes* in all of the groups (Fig. 5A). *Bacteroidetes* was the most abundant phylum in the RC, HF and FO groups, whereas *Firmicutes* was the most abundant in the SMO group. The relative abundance of *Bacteroidetes* and *Firmicutes* was almost equal in the OL group. The relative abundance of *Bacteroidetes* and *Firmicutes*, as well as their ratio, varied significantly among the five groups (Fig. 5B–D). The relative abundance of *Bacteroidetes* was significantly lower in the HF group than in the RC group. It was significantly increased after the obese mice were fed with FO and significantly lower in the SMO and OL groups than in the RC and HF groups. The relative abundance of *Firmicutes* in the HF group was slightly higher than that in the RC group, with no statistical difference. It was significantly lower in the FO group, while higher in the SMO group than in the HF group. The ratio of *Bacteroidetes* to *Firmicutes* was significantly lower in the HF group than in the RC group. Compared with the HF group, the ratio was significantly increased in the FO group and
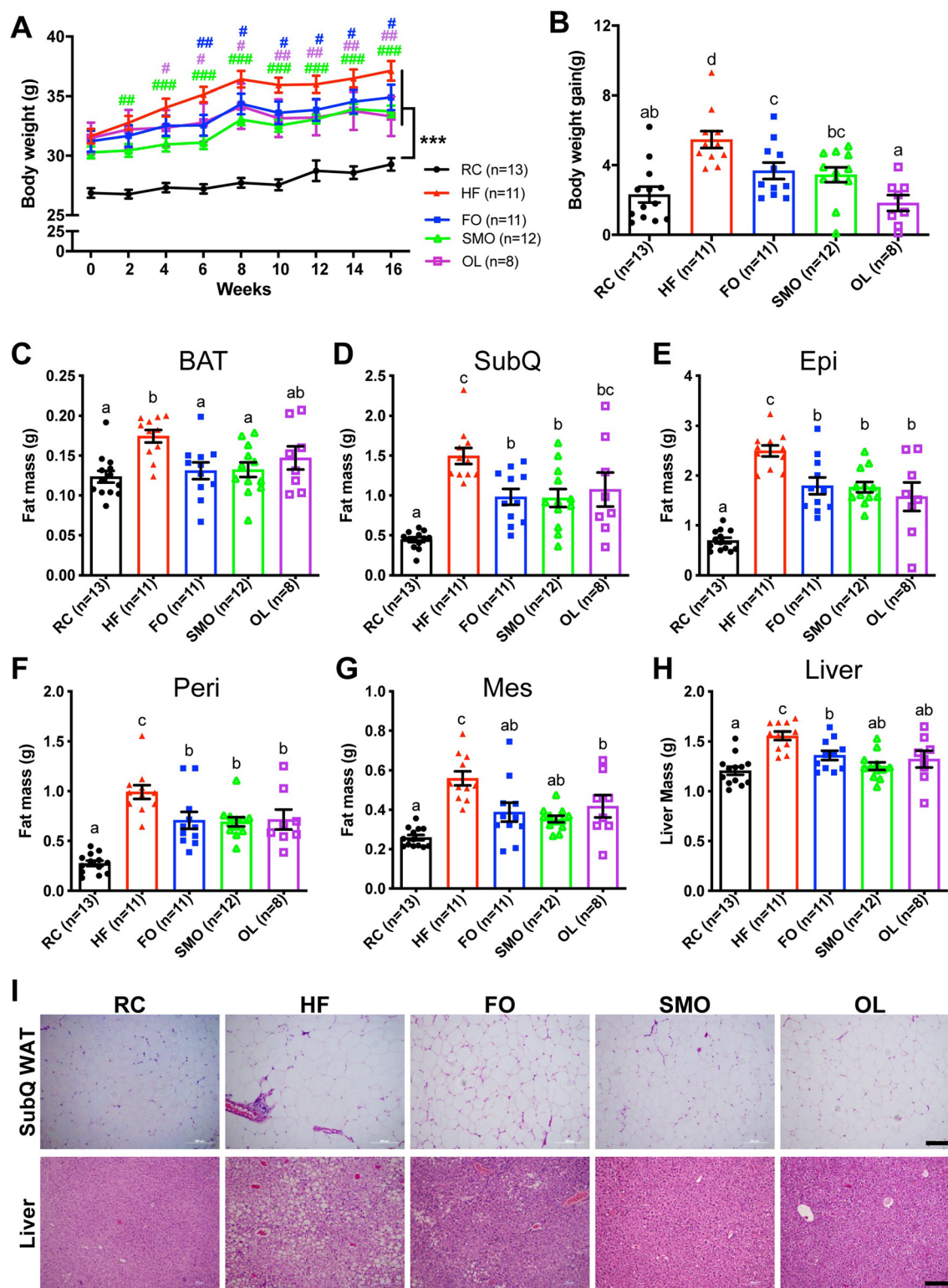
Fig. 2 Effects of SMO on body weight and lipid accumulation in the adipose tissues and the liver of HFD-induced obesity mice. (A) The growth curve of mice during the treatment. *** ($P \leq 0.001$) compared with the RC group; "#" ($P \leq 0.05$), "##" ($P \leq 0.01$), and "###" ($P \leq 0.001$) compared with the HF group. (B) The body weight gain of mice after the treatment. (C)–(G) Weights of adipose tissues: BAT, brown adipose tissue; SubQ, sub-cutaneous white adipose tissue; Epi, epididymal white adipose tissue; Peri, perinephric white adipose tissue; Mes, mesenteric white adipose tissue. (H) Weight of the liver. (I) H&E staining of the SubQ WAT and liver. Scale bar = 200 μm. Different lowercase letters above the error bars indicate significant differences among groups.
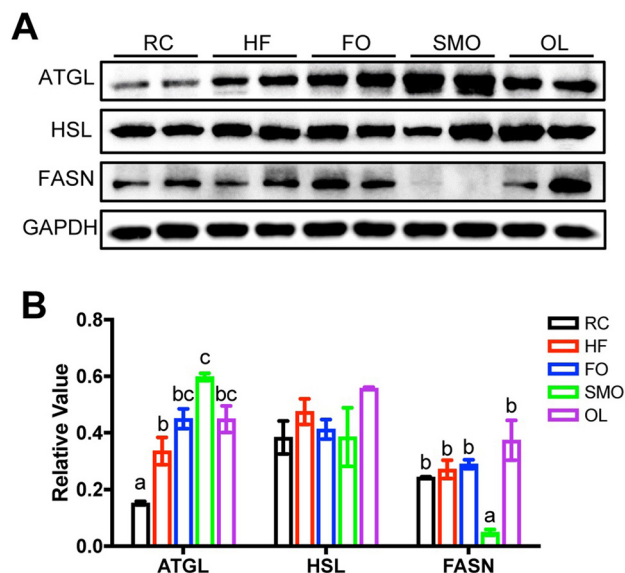
Fig. 3 The levels of proteins involved in lipid metabolism in adipose tissue. (A) Western blot analysis of the protein levels. (B) The density of bands was normalized to GAPDH. Different lowercase letters above the error bars indicate significant differences among groups.
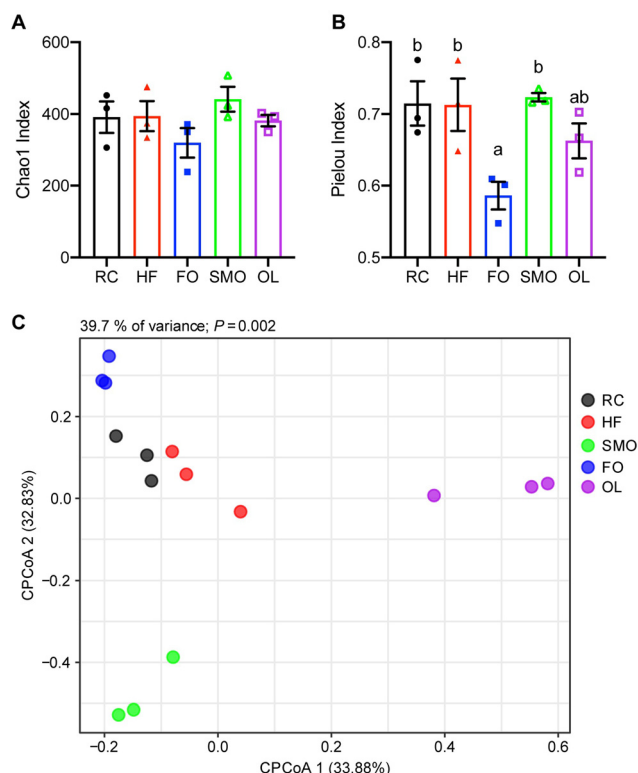

Fig. 4 Analysis of the alpha-diversity and the beta-diversity of gut bacterial communities in different groups. (A) Chao1 index, (B) Pielou index and (C) the CPCoA plot of bacterial communities in different samples. Different lowercase letters above the error bars indicate significant differences among groups.

decreased in the SMO group. The relationship between the phylum and fatty acids in the FO and SMO groups was analyzed (Fig. 5E). Fatty acids were significantly correlated with *Firmicutes*, *Bacteroidetes*, and *Proteobacteria*. DHA was positively correlated with *Firmicutes* and *Proteobacteria*, and EPA as well as SFAs and MUFAs were positively correlated with *Bacteroidetes*.

The ternary plot displayed the differently prevalent bacterial species among the FO, SMO, and OL groups (Fig. S2†). It was found that many species belonging to the order *Bacteroidales* were prevalent in the FO group. Those belonging to *Clostridiales* were abundant and ubiquitous in the SMO group, and *Verrucomicrobiales* was the most abundant bacteria prevalent in the OL group. The volcano plot was established at the OTU level to compare the variance of the gut bacterial communities between the HF group and each of the SMO, FO and OL groups (Fig. 5F), and the taxonomic information of the OTUs is listed in Table S2.† Overall, compared with the HF group, the number of the differentially distributed OTUs was highest in the SMO group and lowest in the FO group. In the SMO group, the abundances of nine OTUs were significantly increased, and those of 20 OTUs were significantly decreased. In the FO group, five OTUs were significantly enriched, and nine OTUs were significantly downregulated. In the OL group, the significantly upregulated and downregulated OTUs were eight and ten, respectively. Based on the significantly changed OTUs identified by the volcano plot, a heatmap was plotted to reveal the changes in these OTUs in the gut of mice treated with different diets (Fig. 5G). It was shown that several OTUs belonging to *Ruminococcaceae* (OTUs 111, 173, 110, and 114) and *Lachnospiraceae* (OTUs 149, 162, and 8) were significantly enriched, and those belonging to *Parasutterella* (OTUs 69, 94, and 105) were significantly downregulated in the SMO group compared with the HF group. In the FO group, the abundances of OTUs 21 and 24, OTU 52, OTU 198 and OTU 201 were affiliated with *Alistipes*, Rikenellaceae RC9 gut group, *Vibrio* and *Flavobacteriaceae*, respectively, and were significantly higher than those in the HF group. Several OTUs belonging to *Clostridia* (OTUs 17, 200, 57, 116, 168 and 203), *Parasutterella* (OTUs 97 and 72) and *Faecalibaculum* (OTU 63) were significantly downregulated. In the OL group, the abundances of OTUs belonging to *Alistipes* (OTU 204), *Akkermansia* (OTU 3) and *Lactobacillus* (OTU 12) were significantly increased.

3.7. Correlation of gut bacterial species with obesity-related indices

To investigate the correlations between SMO modulated gut microbiota and obesity, Pearson's correlation was analyzed based on the differently prevalent OTUs and obesity-related indices in the HF and SMO groups (Fig. S3†). The result revealed that OTUs 21 and 24 (*Alistipes*) and OTU 114 (*Anaerotruncus*) were significantly negatively correlated with almost all the obesity-related indices, while OTUs 166 and 20 that belong to *Muribaculaceae* showed a strong positive correlation with obesity-related indices.
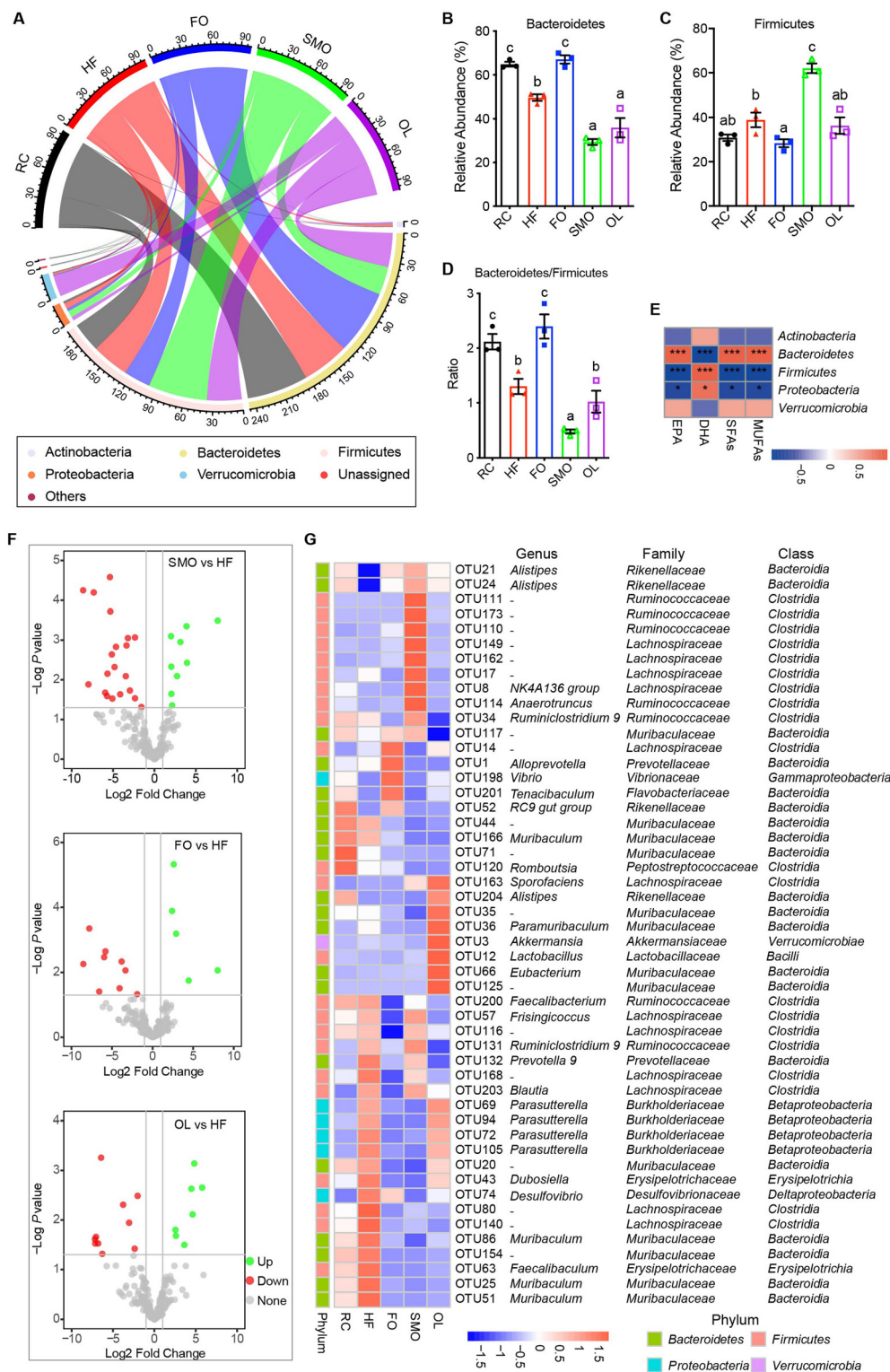
Fig. 5 Taxonomic composition of bacterial communities in different groups. (A) Chordal graph illustrating the bacterial community composition. (B)–(D) Changes in the relative abundances of *Bacteroidetes* (B) and *Firmicutes* (C) as well as their ratio (D). (E) Correlation between the bacterial phylum and fatty acid in the FO and SMO groups. (F) Volcano plots illustrating the differences in OTUs between the HF group and each of the SMO, FO, and OL groups. (G) Heatmap illustrating the variations in the significantly differential OTUs among different groups. Different lowercase letters above the error bars indicate significant differences among groups.

3.8. Phenotypic changes in gut bacterial communities under different treatments

BugBase was used to predict the high-level phenotypes of the gut bacterial community. The relative abundance of aerobic and anaerobic bacteria was significantly higher and lower, respectively, in the OL groups than in the other groups, and

there was no significant difference among the RC, HF, FO, and SMO groups (Fig. 6A). In addition, the relative abundance of Gram-negative bacteria was significantly lower, and Gram-positive bacteria significantly higher in the SMO group than in the other groups (Fig. 6A), which was consistent with the increased abundance of *Firmicutes* in the SMO group. Furthermore, the functional pathways of gut microbiota were predicted with
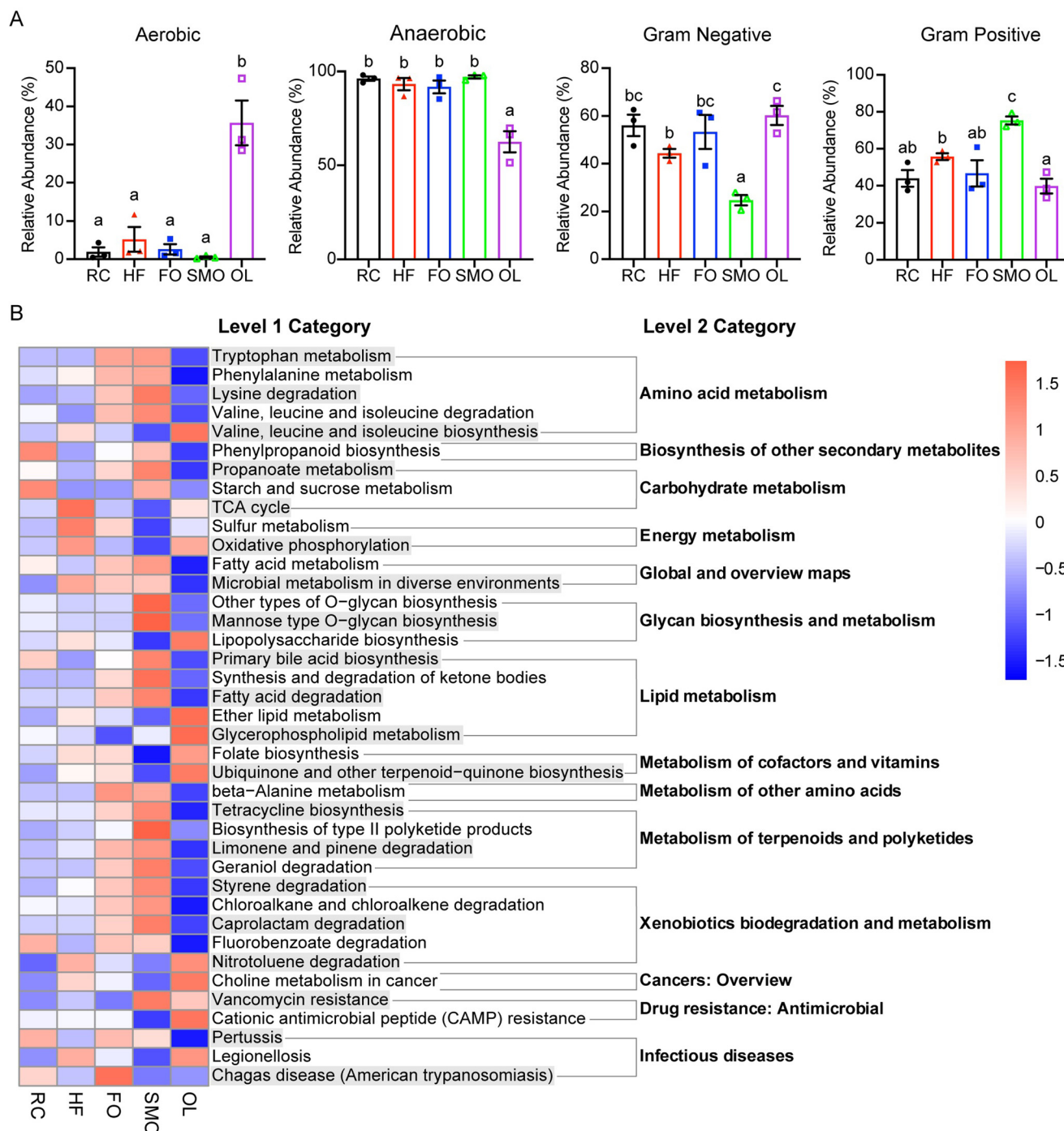

Fig. 6 Prediction of the phenotypes and functions of the gut bacterial community in different groups. (A) Relative abundances of four potential phenotypes predicted by BugBase. (B) Heatmap showing the relative abundances of the KEGG pathways related to metabolism and disease inferred by Tax4Fun2.

Tax4Fun2. It was found that 45 pathways at the level 1 KEGG category were significantly distributed among the five groups (Fig. S4†). Based on these pathways, the relative abundances and distributions of those related to metabolism and disease are shown in the heatmap (Fig. 6B). The results indicated that the high-fat diet decreased the abundances of two carbohydrate metabolism pathways and increased the abundances of TCA cycle and two energy metabolism pathways compared with the RC group. The abundances of most of the metabolism-related pathways, including amino acid, carbohydrate and lipid metabolisms, were enriched in the oil-treated groups, especially in the SMO group. However, the abundances of those pathways were decreased in the OL group. Notably, the fatty acid degradation pathway, the propanoate metabolism pathway that is involved in the production of short-chain fatty acids (SCFAs) and the bile acid biosynthesis pathway were all significantly enriched, while the lipopolysaccharide (LPS) biosynthesis pathway was significantly inhibited in the SMO group. Moreover, FO, SMO and Orlistat decreased the abundances of the TCA cycle and the sulfur metabolism and oxidative phosphorylation-related pathways, which were increased after high-fat treatment, with the SMO being the most effective. In addition, the SMO decreased the abundances of several disease-related pathways, while the abundances of most of the disease-related pathways were increased in the OL group.

3.9 Effects of SMO on the colonic mucosal barrier

The intestinal mucosal barrier is of significance in protecting epithelial cells from invasion, and gut microbiota play important roles in maintaining mucosal barrier health. In this study, the effect of different treatments on colonic mucosa was observed. Compared with the RC group, the HFD-induced mice had rough crypt surfaces and loss of crypt and goblet cells, while both FO and SMO restored the impaired mucosa, except for that in mice of the OL group, which was characterized by an uneven crypt, fewer crypt and goblet cells, and even inflammatory cell infiltration (Fig. 7A). Moreover, levels of tight junction proteins (Occludin and Claudin-1) were detected in different groups (Fig. 7B and C). Compared with the RC group, both Occludin and Claudin-1 were reduced in the HF group, while SMO and FO restored their expression levels. However, the levels of Occludin and Claudin-1 were still low in the OL group.

4. Discussion

EPA and DHA are two main bioactive forms of omega-3 PUFAs. Although omega-3 PUFAs are considered agents that reduce obesity, omega-3 PUFAs used in previous studies were mainly a mixture of EPA and DHA. Commercial fish oil supplements are also characterized by higher EPA/DHA ratios. EPA and DHA may result in different metabolic effects owing to their different molecular structures.[25] In our study, the high-DHA SMO was found to alleviate obesity, hyperglycemia and hyperli-

pidemia in obese mice as efficiently as commercial fish oil and Orlistat. These effects of SMO were consistent with studies on omega-3 PUFAs from fish and microalgae,[9,11,26–29] and our previous study about the preventative effects of SMO on obesity.[14] Notably, SMO exhibits a body-weight-reducing effect earliest and has stronger capabilities for reducing serum TG and fatty liver than commercial fish oil, which is probably attributed to its robust capability in inducing the expression of the lipolysis-related gene and reducing the expression of the lipogenesis-related gene in obese mice.

Gut microbiota play a significant role in regulating host nutrient acquisition and energy metabolism.[15,30] Nevertheless, gut microbiota-modulating effects of SMO were unclear. Richness and evenness, which indicate a bacterial community's functional stability, are regarded as important measures of community biodiversity.[31] The risk of losing functionality is higher for an uneven community than for an even community.[32] In the present study, the Chao1 richness and especially the Pielou evenness indices were decreased in the gut of FO-treated obese mice, suggesting an unstable community after FO treatment. *Bacteroidetes*, *Firmicutes* and their ratio (B/F) have been implicated as being closely associated with obesity.[33] We found that HFD obese mice were characterized by a significant decrease in the B/F ratio, while the effect of FO and SMO on the B/F ratio was the opposite. The FO significantly increased the B/F ratio reduced by HFD, which was consistent with previous studies regarding the effects of fish oil or omega-3 fatty acids on gut microbiota.[25,34] Nevertheless, SMO significantly decreased the B/F ratio. Actually, these changes at the phylum level cannot be currently considered as salient biomarkers for obesity.[30] The different responses of gut microbiota probably result from the different compositions of omega-3 PUFAs in FO and SMO, as the major omega-3 PUFAs in FO used in this study are EPA (19.3%) and DHA (16.7%), while the purified SMO is dominated by DHA (97.8%). It has been considered that EPA and DHA exert different effects on gut microbiota in different animal models.[25,35,36] Both EPA and DHA exhibit antibacterial activities. However, Gram-negative bacteria are more sensitive to DHA.[37] In the present study, DHA also showed a significant positive correlation with Gram-positive *Firmicutes*, and the lower level of Gram-negative *Bacteroidetes* and higher level of *Firmicutes* in the SMO group are probably attributed to their higher DHA content. At lower taxonomic levels, it was found that several OTUs affiliating with *Alistipes*, *Lachnospiraceae* and *Ruminococcaceae* were negatively correlated with obesity in the present study. These species are SCFAs-producing bacteria that can regulate inflammation and metabolism,[38,39] and omega-3 PUFAs have been found to induce gut SCFAs-producing bacteria.[40,41] The higher abundance of these bacteria in the SMO group suggested that SMO improved the metabolic capability of gut microbiota in obese mice. In the FO group, the abundance of SCFAs-producing *Alistipes* and *Rikenellaceae RC9* was increased compared with the HF group. Meanwhile, the relative abundance of *Vibrio* and *Desulfovibrio* was higher than those in the SMO and OL groups. *Vibrio* is a well-known opportunistic pathogen and
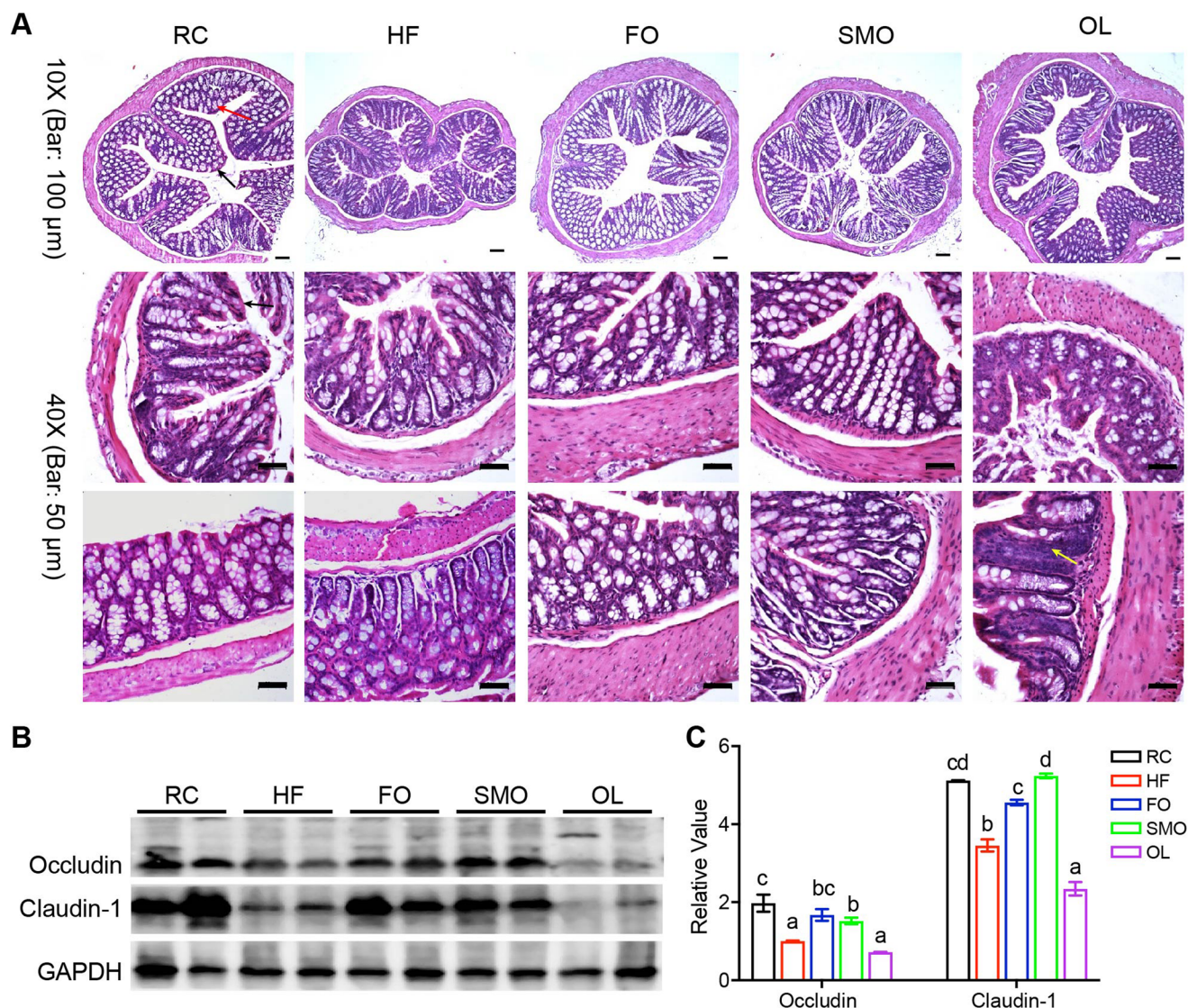
Fig. 7 Effects of different treatments on the colonic mucus barrier. (A) H&E staining of the colon. Black arrow: Crypt surface. Red arrow: Goblet cells. Yellow arrow: Inflammatory cell infiltration. (B) Western blot analysis of the protein levels of Occludin and Claudin-1. (C) Relative levels of Occludin and Claudin-1 normalized to GAPDH. Different lowercase letters above the error bars indicate significant differences among groups.

Desulfovibrio is a typical inflammatory and obesity-promoting bacterium that can produce genotoxic hydrogen sulfide (H$_2$S) gas leading to higher intestinal permeability.[42] In our present study, *Desulfovibrio* was enriched in the HF group. Although its abundance was reduced in both the FO and SMO groups, SMO showed a stronger inhibitory effect, which was in line with the report that a high level of DHA in fish oil efficiently inhibits *Desulfovibrio*.[25] The higher level of *Desulfovibrio* in the FO group might inhibit its obesity-reducing effect, compared with the SMO. Although OL treatment enriched several probiotics, such as *Akkermansia* and *Lactobacillus* that are negatively correlated with obesity,[42,43] several *Parasutterella* were also enriched. It has been previously found that *Parasutterella* is associated with the genesis and development of irritable bowel syndrome (IBS), Crohn's disease, and hypertriglyceridemia-

related acute necrotizing pancreatitis.[44–46] Overall, SMO can increase the abundance of several beneficial bacteria and inhibit the growth of several pathogens, suggesting that it is more beneficial for gut health.

The change in the bacterial composition reflected its functional variation in the gut of treated mice. The gut microbiome is predominantly composed of facultative and strictly anaerobic bacteria. The expansion of aerobic bacteria is strongly linked to various diseases, such as chronic pancreatitis.[47] Therefore, the overgrowth of aerobic bacteria in the OL group indicated the dysbiosis of the gut microbiota after Orlistat administration. Based on the KEGG pathway prediction, the carbohydrate metabolism and energy metabolism of the gut microbiota were disturbed by HFD compared with the RC group, which might contribute to HFD-induced obesity. SMO

was found to recover these pathway abundances most efficiently. Microbial metabolites are significant in regulating the host's metabolism. In this study, SMO was found to significantly increase the abundances of fatty acid degradation pathway and SCFAs-producing related pathway, which is helpful for body-weight management. Compared with the HF group, the altered bacterial metabolic pathway in the gut of the FO and SMO groups may contribute to lipid metabolism in adipose tissue. The upregulation of the tryptophan-derived microbial metabolite indole has been shown to reduce body-weight gain by inducing miR-181 expression in white adipocytes.[48] The bacterial tryptophan metabolism pathway was induced in the FO- and SMO-treated gut, which may contribute to their weight-loss effects. Moreover, compared with the HF group, the gut bacteria in the OL group showed the highest abundance of LPS biosynthesis pathways, while that in the SMO group was the lowest. It has been reported that activating the LPS-TLR4 axis inhibits adipose tissue browning and increases fat accumulation by inducing lipogenesis.[49,50] Therefore, the lowest level of LPS biosynthesis pathways in the gut of the SMO group may contribute to the inhibition of lipogenesis-related genes and thus reduce the fat mass. Moreover, bile acids are important regulators in lipid metabolism and mediate the interaction between gut microbiota and host through gut–liver and gut–adipose tissue axes.[51] Although the bile acid biosynthesis pathway was enriched in both the FO and SMO groups compared with the HF group, its abundance was higher in the SMO group than in the FO group, which may also lead to the effective improvement of lipid metabolism in SMO-treated HFD mice. However, most metabolic pathways were inhibited by Orlistat, suggesting the functional dysbiosis of gut microbiota by Orlistat. Overall, SMO can improve gut microbiota metabolism, which is possible to associate with the improvement in lipid metabolism in adipose tissue.

Gut microbiota are closely associated with intestinal mucus health. Intestinal crypt goblet cells contribute greatly to mucus barrier formation, and tight junction proteins are essential for intestinal permeability. Previous studies have shown that omega-3 PUFAs can alleviate colonic mucus disruption in colitis mouse models.[52] Although EPA and DHA were reported to have different effects on relieving mucus barrier disruption in the colitis model,[52] both SMO and FO effectively recovered the colonic mucus layer damaged by HFD in our study. The differences may be due to the different animal models used in our study and the previous ones where the colonic inflammation was much more serious. In addition, the expression of tight junction proteins was reduced in the HF group, which was in line with previous studies.[53] We found that SMO and FO restored the expression of tight junction proteins rather than OL. Microbial SCFAs production is essential for gut integrity and health as well as the regulation of tight junction proteins.[54,55] The effective mucus repair by SMO and FO may be attributed to the higher levels of SCFAs-producing bacteria and the related metabolic pathway. In addition, the highest level of LPS biosynthesis pathway may lead to gut inflammation in the OL group.

5. Conclusions

SMO has comparable weight-loss effects with commercial fish oil and Orlistat, and it is even better in terms of onset time as well as serum TG and fatty liver reduction. In addition, SMO and FO exert different gut microbiota regulation effects owing to their different compositions. SMO can maintain the stability of gut microbiota, selectively increase the relative abundance of beneficial bacteria, decrease that of pathogenic bacteria, and improve gut metabolism. Our results suggested that SMO is a better potential functional dietary supplement for treating obesity, and the detailed mechanisms involved in weight-loss effects mediated by the gut microbiota regulation of SMO need to be deeply studied.

Author contributions

Liyuan Ran: Investigation, conceptualization, methodology, funding acquisition, validation, and writing—original draft. Jinhui Yu: Investigation, validation, and writing—review and editing. Rui Ma: Investigation and writing—review and editing. Qing Yao: Investigation, writing—review and editing. Mingjie Wang: Investigation and writing—review and editing. Yuping Bi: Resources, writing—review and editing. Zichao Yu: Conceptualization, investigation, methodology, validation, supervision, writing—original draft and writing—review and editing. Yingjie Wu: Funding acquisition, methodology, validation, formal analysis, project administration, and writing—review and editing.

Conflicts of interest

There are no conflicts to declare.

Acknowledgements

References

1 K. Van Raemdonck, S. Umar, Z. Szekanecz, R. K. Zomorrodi and S. Shahrara, Impact of obesity on autoimmune arthritis and its cardiovascular complications, *Autoimmun. Rev.*, 2018, **17**, 821–835.

2 J. A. J. Martyn, M. Kaneki, S. Yasuhara, D. S. Warner and M. A. Warner, Obesity-induced insulin resistance and hyperglycemia: etiologic factors and molecular mechanisms, *Anesthesiology*, 2008, **109**, 137–148.

3   M. E. Rinella, Nonalcoholic fatty liver disease: a systematic review, *J. Am. Med. Assoc.*, 2015, **313**, 2263–2273.

4   E. Nehus, Obesity and chronic kidney disease, *Curr. Opin. Pediatr.*, 2018, **30**, 241–246.

5   M. D. Jensen, D. H. Ryan, K. A. Donato, C. M. Apovian, J. D. Ard, A. G. Comuzzie, F. B. Hu, V. S. Hubbard, J. M. Jakicic, R. F. Kushner, C. M. Loria, B. E. Millen, C. A. Nonas, F. X. Pi-Sunyer, J. Stevens, V. J. Stevens, T. A. Wadden, B. M. Wolfe and S. Z. Yanovski, Executive summary: Guidelines (2013) for the management of overweight and obesity in adults, *Obesity*, 2014, **22**, S5–S39.

6   J. G. Kang and C.-Y. Park, Anti-obesity drugs: a review about their effects and safety, *Diabetes Metab. J.*, 2012, **36**, 13.

7   A. Sato, H. Kawano, T. Notsu, M. Ohta, M. Nakakuki, K. Mizuguchi, M. Itoh, T. Suganami and Y. Ogawa, Antiobesity effect of eicosapentaenoic acid in high-fat/high-sucrose diet–induced obesity: importance of hepatic lipogenesis, *Diabetes*, 2010, **59**, 2495–2504.

8   H.-K. Kim, M. Della-Fera, J. Lin and C. A. Baile, Docosahexaenoic acid inhibits adipocyte differentiation and induces apoptosis in 3T3-L1 preadipocytes, *J. Nutr.*, 2006, **136**, 2965–2969.

9   L. M. Neff, J. Culiner, S. Cunningham-Rundles, C. Seidman, D. Meehan, J. Maturi, K. M. Wittkowski, B. Levine and J. L. Breslow, Algal docosahexaenoic acid affects plasma lipoprotein particle size distribution in overweight and obese adults, *J. Nutr.*, 2011, **141**, 207–213.

10 R.-E. Go, K.-A. Hwang, G.-T. Park, H.-M. Lee, G.-A. Lee, C.-W. Kim, S.-Y. Jeon, J.-W. Seo, W.-K. Hong and K.-C. Choi, Effects of microalgal polyunsaturated fatty acid oil on body weight and lipid accumulation in the liver of C57BL/6 mice fed a high fat diet, *J. Biomed. Res.*, 2016, **30**, 234.

11 J.-S. Yook, K.-A. Kim, J. E. Park, S.-H. Lee and Y.-S. Cha, Microalgal oil supplementation has an anti-obesity effect in C57BL/6J mice fed a high fat diet, *Prev. Nutr. Food Sci.*, 2015, **20**, 230.

12 T. Komprda, Z. Sladek, O. Škultéty, S. Křížková, V. Rozikova, B. Němcová, T. Šustrová and M. Valova, Effect of dietary *Schizochytrium* microalga oil on selected markers of low–grade inflammation in rats, *J. Anim. Physiol. Anim. Nutr.*, 2016, **100**, 1169–1178.

13 T. Komprda, O. Škultéty, S. Křížková, G. Zorníková, V. Rozíková and R. Krobot, Effect of dietary *Schizochytrium* microalga oil and fish oil on plasma cholesterol level in rats, *J. Anim. Physiol. Anim. Nutr.*, 2015, **99**, 308–316.

14 J. Yu, Y. Ma, J. Sun, L. Ran, Y. Li, N. Wang, T. Yu, W. Gao, W. Jia and R. Jiang, Microalgal oil from *Schizochytrium* sp. prevents HFD-induced abdominal fat accumulation in mice, *J. Am. Coll. Nutr.*, 2017, **36**, 347–356.

15 F. Sommer and F. Bäckhed, The gut microbiota—masters of host development and physiology, *Nat. Rev. Microbiol.*, 2013, **11**, 227–238.

16 C. L. Boulangé, A. L. Neves, J. Chilloux, J. K. Nicholson and M.-E. Dumas, Impact of the gut microbiota on inflammation, obesity, and metabolic disease, *Genome Med.*, 2016, **8**, 42.

17 G. Musso, R. Gambino and M. Cassader, Gut microbiota as a regulator of energy homeostasis and ectopic fat deposition: mechanisms and implications for metabolic disorders, *Curr. Opin. Lipidol.*, 2010, **21**, 76–83.

18 H. Watson, S. Mitra, F. C. Croden, M. Taylor, H. M. Wood, S. L. Perry, J. A. Spencer, P. Quirke, G. J. Toogood and C. L. Lawton, A randomised trial of the effect of omega-3 polyunsaturated fatty acid supplements on the human intestinal microbiota, *Gut*, 2018, **67**, 1974–1983.

19 Y. Wu, C. Liu, H. Sun, A. Vijayakumar, P. R. Giglou, R. Qiao, J. Oppenheimer, S. Yakar and D. LeRoith, Growth hormone receptor regulates β cell hyperplasia and glucose-stimulated insulin secretion in obese mice, *J. Clin. Invest.*, 2011, **121**, 2422–2426.

20 F. Pacifici, R. Arriga, G. P. Sorice, B. Capuani, M. G. Scioli, D. Pastore, G. Donadel, A. Bellia, S. Caratelli and A. Coppola, Peroxiredoxin 6, a novel player in the pathogenesis of diabetes, *Diabetes*, 2014, **63**, 3210–3220.

21 E. Bolyen, J. R. Rideout, M. R. Dillon, N. A. Bokulich, C. C. Abnet, G. A. Al-Ghalith, H. Alexander, E. J. Alm, M. Arumugam, F. Asnicar and J. G. Caporaso, Reproducible, interactive, scalable and extensible microbiome data science using QIIME 2, *Nat. Biotechnol.*, 2019, **37**, 852–857.

22 T. Ward, J. Larson, J. Meulemans, B. Hillmann, J. Lynch, D. Sidiropoulos, J. R. Spear, G. Caporaso, R. Blekhman, R. Knight, R. Fink and D. Knights, BugBase predicts organism-level microbiome phenotypes, *BioRxiv*, 2017, 133462.

23 F. Wemheuer, J. A. Taylor, R. Daniel, E. Johnston, P. Meinicke, T. Thomas and B. Wemheuer, Tax4Fun2: prediction of habitat-specific functional profiles and functional redundancy based on 16S rRNA gene sequences, *Environ. Microbiome*, 2020, **15**, 1–12.

24 N. Segata, J. Izard, L. Waldron, D. Gevers, L. Miropolsky, W. S. Garrett and C. Huttenhower, Metagenomic biomarker discovery and explanation, *Genome Biol.*, 2011, **12**, 1–18.

25 J. Zhang, C. Yi, J. Han, T. Ming, J. Zhou, C. Lu, Y. Li and X. Su, Novel high–docosahexaenoic–acid tuna oil supplementation modulates gut microbiota and alleviates obesity in high–fat diet mice, *Food Sci. Nutr.*, 2020, **8**, 6513–6527.

26 G. Andersen, K. Harnack, H. F. Erbersdobler and V. Somoza, Dietary eicosapentaenoic acid and docosahexaenoic acid are more effective than alpha-linolenic acid in improving insulin sensitivity in rats, *Ann. Nutr. Metab.*, 2008, **52**, 250–256.

27 T. C. L. Bargut, A. C. A. G. Silva-e, V. Souza-Mello, C. A. Mandarim-de-Lacerda and M. B. Aguila, Mice fed fish oil diet and upregulation of brown adipose tissue thermogenic markers, *Eur. J. Nutr.*, 2016, **55**, 159–169.

28 A. González-Périz, R. Horrillo, N. Ferre, K. Gronert, B. Dong, E. Morán-Salvador, E. Titos, M. Martínez-Clemente, M. López-Parra and V. Arroyo, Obesity–induced insulin resistance and hepatic steatosis are alleviated by ω–

3 fatty acids: a role for resolvins and protectins, *FASEB J.*, 2009, **23**, 1946–1957.

29 M. Bhaswant, H. Poudyal and L. Brown, Mechanisms of enhanced insulin secretion and sensitivity with n-3 unsaturated fatty acids, *J. Nutr. Biochem.*, 2015, **26**, 571–584.

30 P. Gérard, Gut microbiota and obesity, *Cell. Mol. Life Sci.*, 2016, **73**, 147–162.

31 A. Purvis and A. Hector, Getting the measure of biodiversity, *Nature*, 2000, **405**, 212–219.

32 P. Balvanera, C. Kremen and M. Martínez-Ramos, Applying community structure analysis to ecosystem function: examples from pollination and carbon storage, *Ecol. Appl.*, 2005, **15**, 360–375.

33 P. J. Turnbaugh, R. E. Ley, M. A. Mahowald, V. Magrini, E. R. Mardis and J. I. Gordon, An obesity-associated gut microbiome with increased capacity for energy harvest, *Nature*, 2006, **444**, 1027–1031.

34 C. Parolini, Effects of fish n-3 PUFAs on intestinal microbiota and immune system, *Mar. Drugs*, 2019, **17**, 374.

35 R. Hosomi, A. Matsudo, K. Sugimoto, T. Shimono, S. Kanda, T. Nishiyama, M. Yoshida and K. Fukunaga, Dietary Eicosapentaenoic Acid and Docosahexaenoic Acid Ethyl Esters Influence the Gut Microbiota and Bacterial Metabolites in Rats, *J. Oleo Sci.*, 2021, **70**, 1469–1480.

36 P. Zhuang, H. Li, W. Jia, Q. Shou, Y. e. Zhu, L. Mao, W. Wang, F. Wu, X. Chen, X. Wan, Y. Wu, X. Liu, Y. Li, F. Zhu, L. He, J. Chen, Y. Zhang and J. Jiao, Eicosapentaenoic and docosahexaenoic acids attenuate hyperglycemia through the microbiome-gut-organs axis in db/db mice, *Microbiome*, 2021, **9**, 185.

37 S. Y. Shin, V. K. Bajpai, H. R. Kim and S. C. Kang, Antibacterial activity of bioconverted eicosapentaenoic (EPA) and docosahexaenoic acid (DHA) against foodborne pathogenic bacteria, *Int. J. Food Microbiol.*, 2007, **113**, 233–236.

38 A. Benítez-Páez, E. M. Gómez del Pugar, I. López-Almela, Á. Moya-Pérez, P. Codoñer-Franch and Y. Sanz, Depletion of *Blautia* species in the microbiota of obese children relates to intestinal inflammation and metabolic phenotype worsening, *mSystems*, 2020, **5**, e00857-19.

39 C. Kang, B. Wang, K. Kaliannan, X. Wang, H. Lang, S. Hui, L. Huang, Y. Zhang, M. Zhou and M. Chen, Gut microbiota mediates the protective effects of dietary capsaicin against chronic low-grade inflammation and associated obesity induced by high-fat diet, *mBio*, 2017, **8**, e00470-17.

40 A. D. Andersen, L. Mølbak, K. F. Michaelsen and L. Lauritzen, Molecular fingerprints of the human fecal microbiota from 9 to 18 months old and the effect of fish oil supplementation, *J. Pediatr. Gastroenterol. Nutr.*, 2011, **53**, 303–309.

41 H. Watson, S. Mitra, F. C. Croden, M. Taylor, H. M. Wood, S. L. Perry, J. A. Spencer, P. Quirke, G. J. Toogood, C. L. Lawton, l. Dye, P. M. loadman and M. A. Hull, A randomised trial of the effect of omega-3 polyunsaturated fatty acid supplements on the human intestinal microbiota, *Gut*, 2018, **67**, 1974–1983.

42 M. W. Rohr, C. A. Narasimhulu, T. A. Rudeski-Rohr and S. Parthasarathy, Negative effects of a high-fat diet on intestinal permeability: a review, *Adv. Nutr.*, 2020, **11**, 77–91.

43 F. J. Verdam, S. Fuentes, C. de Jonge, E. G. Zoetendal, R. Erbil, J. W. Greve, W. A. Buurman, W. M. de Vos and S. S. Rensen, Human intestinal microbiota composition is associated with local and systemic inflammation in obesity, *Obesity*, 2013, **21**, E607–E615.

44 Y. J. Chen, H. Wu, S. D. Wu, N. Lu, Y. T. Wang, H. N. Liu, L. Dong, T. T. Liu and X. Z. Shen, Parasutterella, in association with irritable bowel syndrome and intestinal chronic inflammation, *J. Gastroenterol. Hepatol.*, 2018, **33**, 1844–1852.

45 R. J. Chiodini, S. E. Dowd, W. M. Chamberlin, S. Galandiuk, B. Davis and A. Glassing, Microbial population differentials between mucosal and submucosal intestinal tissues in advanced Crohn's disease of the ileum, *PLoS One*, 2015, **10**, e0134382.

46 C. Huang, J. Chen, J. Wang, H. Zhou, Y. Lu, L. Lou, J. Zheng, L. Tian, X. Wang and Z. Cao, Dysbiosis of intestinal microbiota and decreased antimicrobial peptide level in paneth cells during hypertriglyceridemia-related acute necrotizing pancreatitis in rats, *Front. Microbiol.*, 2017, **8**, 776.

47 M.-M. Han, X.-Y. Zhu, Y.-F. Peng, H. Lin, D.-C. Liu and L. Li, The alterations of gut microbiota in mice with chronic pancreatitis, *Ann. Transl. Med.*, 2019, **7**, 464.

48 A. T. Virtue, S. J. McCright, J. M. Wright, M. T. Jimenez, W. K. Mowel, J. J. Kotzin, L. Joannas, M. G. Basavappa, S. P. Spencer, M. L. Clark, S. H. Eisennagel, A. Williams, M. Levy, S. Manne, S. E. Henrickson, E. J. Wherry, C. A. Thaiss, E. Elinav and J. Henao-Mejia, The gut microbiota regulates white adipose tissue inflammation and obesity via a family of microRNAs, *Sci. Transl. Med.*, 2019, **11**, eaav1892.

49 C. Chen, S. Fang, H. Wei, M. He, H. Fu, X. Xiong, Y. Zhou, J. Wu, J. Gao, H. Yang and L. Huang, Prevotella copri increases fat accumulation in pigs fed with formula diets, *Microbiome*, 2021, **9**, 175.

50 J. M. Moreno-Navarrete and J. M. Fernandez-Real, The gut microbiota modulates both browning of white adipose tissue and the activity of brown adipose tissue, *Rev. Endocr. Metab. Disord.*, 2019, **20**, 387–397.

51 T. Li and J. Y. Chiang, Bile acid signaling in metabolic disease and drug therapy, *Pharmacol. Rev.*, 2014, **66**, 948–983.

52 J. Fang, Z. Zhang, Y. Cheng, H. Yang, H. Zhang, Z. Xue, S. Lu, Y. Dong, C. Song and X. Zhang, EPA and DHA differentially coordinate the crosstalk between host and gut microbiota and block DSS-induced colitis in mice by a reinforced colonic mucus barrier, *Food Funct.*, 2022, **13**, 4399–4420.

53 M. Rohr, C. Narasimhulu, T. Rudeski-Rohr and S. Parthasarathy, Negative effects of a high-fat diet

on intestinal permeability: A review, *Adv. Nutr.*, 2020, **11**, 77–91.

54 E. Blaak, E. Canfora, S. Theis, G. Frost, A. Groen, G. Mithieux, A. Nauta, K. Scott, B. Stahl, J. van Harsselaar, R. van Tol, E. E. Vaughan and K. Verbeke, Short chain fatty acids in human gut and metabolic health, *Benefic. Microbes*, 2020, **11**, 411–455.

55 D. J. Morrison and T. Preston, Formation of short chain fatty acids by the gut microbiota and their impact on human metabolism, *Gut Microbes*, 2016, **7**, 189–200.